NATIONAL ADVISORY COMMITTEE
FOR AERONAUTICS

2- 6. 53

TECHNICAL MEMORANDUM 1358

CALCULATION OF THE SHAPE OF A TWO-DIMENSIONAL

SUPERSONIC NOZZLE IN CLOSED FORM

By Dante Cunsolo

Translation of "Sul Calcolo in Termini Finiti dell'Effusore
di una Galleria Bidimensionale Supersonica."
L'Aerotecnica, Vol. XXXI, No. 4,
15 August 1951

NACA

Washington
January 1953

NATIONAL ADVISORY COMMITTEE FOR AERONAUTICS

TECHNICAL MEMORANDUM 1358

CALCULATION OF THE SHAPE OF A TWO-DIMENSIONAL

SUPERSONIC NOZZLE IN CLOSED FORM[*]

By Dante Cunsolo

SUMMARY

The idea is advanced of making a supersonic nozzle by producing one, two, or three successive turns of the whole flow; with the result that the wall contour can be calculated exactly by means of the Prandtl-Meyer "Lost Solution."

PURPOSE OF THE INVESTIGATION

The subject matter of this paper is based on the artifice of not letting the expansion waves emanating from one wall of the nozzle be reflected from the opposite side, but of cancelling out their effect by compensating compression waves emanating from this opposite wall. In this way the difficulties attendant upon the intermeshing of the Mach waves are avoided, and it is no longer necessary to integrate the differential equation of the hodograph by recasting it as a finite difference equation, the solution of which is necessarily approximate. The technique illustrated here is nothing more than a quite direct application of the Prandtl-Meyer relationship for flow around a sharp corner. On the basis of this procedure, the calculation of the coordinates of any point on the nozzle contour is independent of that for any other point; that is to say, this way of handling the problem eliminates the lack of precision usually associated with the tail end of the effusor in comparison with the better accuracy at the beginning sections.

In addition, what is of the utmost importance, is that it is not necessary to determine the characteristics of the flow throughout the interior of the nozzle, which leads to a tremendous saving in computational labor, with no deterioration in accuracy.

Theoretical Background

Let us focus our attention now on the expansion which occurs when a stream turns around a sharp corner (see fig. 1). In this figure 1 the following notation applies: μ is the Mach angle, ψ is the complement of the Mach angle, ν is the angle through which the flow has turned as it progresses through its turn around the corner, so that related to this angle of the flow vector is the angle ϑ, which is the angle between the normal to the wall and the radius vector originating at the corner and lying along the points in the flow which have turned through the angle ν.

Then, upon making use of well-known theoretical relationships, it follows that

$$\vartheta = \nu + \psi$$

$$\tan \lambda \vartheta = \lambda \tan \psi$$

$$\lambda = \sqrt{\frac{\gamma - 1}{\gamma + 1}}$$

that is,

$$\nu = \vartheta - \arctan \left(\frac{\tan \lambda \vartheta}{\lambda} \right) \tag{1}$$

Now let us employ this Prandtl-Meyer relationship in order to determine the streamlines of the flow. Let us denote a small lineal element of a streamline by the symbol ds (see fig. 2), and then we may take $d\rho$ and $\rho d\vartheta$ to represent the components of this element in polar coordinates.

Thus one may write:

$$\frac{d\rho}{\rho d\vartheta} = \tan \psi = \frac{\tan \lambda \vartheta}{\lambda}$$

$$\frac{d\rho}{\rho} = \frac{\tan \lambda \vartheta}{\lambda} d\vartheta$$

and consequently

$$\log \rho + \frac{1}{\lambda^2} \log \cos \lambda\vartheta = \text{const.}$$

or

$$\rho(\cos \lambda\vartheta)^{\frac{1}{\lambda^2}} = \text{const.}$$

and upon selection of the value of γ as 1.40, one obtains:

$$\rho \cos^6 \frac{\vartheta}{\sqrt{6}} = \rho_* \tag{2}$$

One of the walls is thus the straight terminal side of the angle of expansion while the other curved wall is defined by means of equation (2) as far out as the location where the angle characterizing the radius vector has ultimately reached the value ϑ_M, at which point the desired Mach number will have been attained. From here on out this wall is also straight and lies parallel to the terminal side of the corner angle. As may be seen from reference to figure 3 the minimum length of effusor which it is possible to have is one which terminates right at the point where the wall stops curving, at which point the very last expansion wave has just been included in the process of executing the total turn. Of course, the depth of the "throat" or critical cross-section is the quantity denoted by ρ_*.

If one wishes to avoid reliance upon a perfectly sharp corner for making the expansion, the two curved walls (see fig. 4) given by the equations

$$\left.\begin{aligned} \rho_1 \cos^6 \frac{\vartheta}{\sqrt{6}} &= \rho_{1*} \\[2em] \rho_2 \cos^6 \frac{\vartheta}{\sqrt{6}} &= \rho_{2*} \end{aligned}\right\} \tag{3}$$

may be employed. Of course, in this case the depth of the throat or critical-cross-section is given by $\rho_* = \rho_{2*} - \rho_{1*}$.

Naturally, for an effusor configuration such as this, the length becomes longer than in the case of the sharp cornered type. The expansion waves which originate from the number 1 wall are exactly counteracted or "swallowed up" when they meet the number 2 wall, without producing any reflection. It is just for this reason, even in case one wants to give some other arbitrary shape to the number 1 wall, that the calculations may be carried out in parametric, but closed-form, provided the Mach lines are maintained as straight lines.

Once it is decided what the shape of the number 1 wall is to be, one may find a value of ν which corresponds to the value of ϑ defining the direction of the Mach wave with reference to the y-axis. This value of ν locates a point with coordinates x_1 and y_1 on the number 1 wall. Consequently, the point lying on the number 2 wall which is marked out by this ϑ-ray will have the coordinates (see fig. 5):

$$\left. \begin{array}{l} x_2 = x_1 + \rho \sin \vartheta \\ \\ y_2 = y_1 - \rho \cos \vartheta \end{array} \right\} \tag{4}$$

where

$$\rho = \rho_* \left(\cos \frac{\vartheta}{\sqrt{6}} \right)^{-6}$$

Obviously it is necessary to have x_1 and y_1 given as functions of ϑ.

Let us follow through on the details in the case where the number 1 wall is taken to be circular, with radius $= \rho_0$. Then the value of ϑ, used as the independent parameter, locates a point with coordinates (see fig. 6):

$$\left. \begin{array}{l} x_1 = \rho_0 \sin \nu \\ \\ y_1 = \rho_* + \rho_0(1 - \cos \nu) \end{array} \right\} \tag{5}$$

wherein the value of ν is given by:

$$\nu = \vartheta - \arctan\left(\sqrt{6}\,\tan\frac{\vartheta}{\sqrt{6}}\right)$$

and the point (x_1, y_1) lies on this ϑ-ray.

Likewise let us examine more fully the case where the number 1 wall is parabolic in shape at the start, with a radius of curvature equal to ρ_0 at the apex of the parabola (see fig. 7). Taking the equation of this parabola to be

$$y = \rho_* + \frac{x^2}{2\rho_0}$$

then its slope is given by

$$\tan\nu = \frac{dy}{dx} = \frac{x}{\rho_0} \tag{6}$$

Consequently, since ϑ is taken as the independent parameter, one obtains

$$\left.\begin{array}{l} \nu = \vartheta - \arctan\left(\sqrt{6}\,\tan\dfrac{\vartheta}{\sqrt{6}}\right) \\[2em] x_1 = \rho_0\,\tan\nu \\[2em] y_1 = \rho_* + \dfrac{\rho_0}{2}\,\tan^2\nu \end{array}\right\} \tag{7}$$

In those cases where the slope dy/dx has more complicated formulations (these would be cases devoid of any practical interest for that matter, in view of the extreme simplicity of construction exemplified by

the contour of the number 1 wall for the configurations just examined in detail) one may still solve the problem, to whatever degree of accuracy is desired, by working with the isocline system:

$$
\left.\begin{array}{c}
v = \vartheta - \arctan \left(\sqrt{6} \ \tan \dfrac{\vartheta}{\sqrt{6}} \right) \\[20pt]
\dfrac{dy}{dx} = \tan v \\[20pt]
y = f(x)
\end{array}\right\} \qquad (8)
$$

which gives the slope of the contour applying at each assigned value of the parameter ϑ. Then, after carrying out this construction, one may find the corresponding values of the coordinates x_2 and y_2, by means of equations (4).

If, however, one insists on having the working section not offset from the axis of the throat, it is necessary to apportion the total angle through which the stream is turned into three pieces. To be more precise, let this total deviation of the flow, corresponding to the ultimate Mach number to be attained, be denoted by v_M. Then the three partial turnings of the flow would be, respectively, an upward turn of amount v'', a downward turn of amount $\dfrac{v_M}{2} = v'' - v'$, and once again an upward turn of amount $\dfrac{v_M}{2} - v' = v_M - v''$. With this arrangement one now has an effusor made up of three expansion regions separated by two sections of uniform flow, wherein the Mach numbers attain the values M' and M'', respectively.

Now let v be the net angle through which the flow has been turned up until the time it has reached a certain location in the effusor; and let ϑ be the angle linked to this value of v by means of the Prandtl-Meyer relationship, equation (1). In addition, let α be the angle swept out by the Mach wave with respect to the y-axis. Then, in the first expansion region, we shall have that $\alpha = \vartheta$ (see figs. 8 and 9). The first Mach wave beginning the second region of expansion will be characterized by the angle $\alpha = 2\psi' - \vartheta'$, while within the second region it will be true that $\alpha = (2\psi' - \vartheta') + (\vartheta - \vartheta') = \vartheta - 2v'$. The last Mach wave ending the second region will be characterized by the

angle $\alpha = \vartheta'' - 2\nu'$, and the first wave beginning the third expansion region is then given by $\alpha = 2\vartheta'' - (\vartheta'' - 2\nu') = 2\vartheta'' - 2\nu'' - \vartheta'' + 2\nu' = \vartheta'' - \nu_M$. For like reasons we have that, within the third region, the Mach angle is given by $\alpha = (\vartheta'' - \nu_M) + (\vartheta - \vartheta'') = \vartheta - \nu_M$. In summary, we have that, in the three expansion regions, the following hold, respectively

$$\left.\begin{array}{l} \alpha = \vartheta \\[2mm] \alpha = \vartheta - 2\nu' \\[2mm] \alpha = \vartheta - \nu_M \end{array}\right\} \qquad\qquad (9)$$

Let us consider what the appropriate relationships are, in the case of a tunnel design such as illustrated in figure 8, wherein the sections of tunnel wall effecting the expansions, that is to say, the convex portions of the wall, consist of circular arcs. For this example the value of ν' must turn out to be calculated in such a way as to make the projection of the broken line A B C D E F G H L upon the y-axis have the value

$$(\text{ABCDEFGHL})_y = \frac{\sigma_M - \sigma_*}{2}$$

where σ_M and σ_* are the widths of the effusor at the very end and at the throat. Writing this condition in explicit form, we obtain the expression

$$\rho_1(1 - \cos\nu') - \frac{\rho_*}{\cos^6 \dfrac{\vartheta'}{\sqrt{6}}} \cos\vartheta' - \rho_2 \cos\nu' +$$

$$\rho_2 \cos\left(\frac{\nu_M}{2} - \nu'\right) + \frac{\rho_*}{\cos^6 \dfrac{\vartheta''}{\sqrt{6}}} \cos(\vartheta'' - 2\nu') -$$

$$\rho_3\left[1 - \cos\left(\frac{\nu_M}{2} - \nu'\right)\right] = \frac{\sigma_M - \sigma_*}{2} \qquad\qquad (10)$$

where ν' and ν'' are the net angles through which the flow has been turned at the end of the first and at the end of the second expansion regions; i.e.,

$$
\left.
\begin{aligned}
\nu' &= \vartheta' - \arctan \frac{\tan \lambda \vartheta'}{\lambda} \\[3mm]
\nu'' &= \nu' + \frac{\nu_M}{2} = \vartheta'' - \arctan \frac{\tan \lambda \vartheta''}{\lambda}
\end{aligned}
\right\}
\tag{11}
$$

In fact, one has in particular that:

$$
(AB)_y = \rho_1
$$

$$
(BC)_y = -\rho_1 \cos \nu'
$$

$$
(CD)_y = -\left| CD \right| \cos \vartheta' = -\rho' \cos \vartheta' = -\frac{\rho_* \cos \vartheta'}{\cos^6 \dfrac{\vartheta'}{\sqrt{6}}}
$$

$$
(DE)_y = -\rho_2 \cos \nu'
$$

$$
(EF)_y = \rho_2 \cos (\overline{EF}, y) = \rho_2 \cos \left(\frac{\nu_M}{2} - \nu' \right)
$$

$$
(FG)_y = \rho'' \cos (\overline{FG}, y) = \frac{\rho_*}{\cos^6 \dfrac{\vartheta''}{\sqrt{6}}} \cos (\vartheta'' - 2\nu')
$$

$$
(GH)_y = \rho_3 \cos \left(\frac{\nu_M}{2} - \nu' \right)
$$

In this case where such circular sections of wall are considered to effect the expansions, it is necessary to utilize equations (5) and (4) (when suitably modified for treatment of the flow in the second and third expansion regions) for getting the solution, but if this circular wall contour is replaced by the curve given by means of equations (3), then this case is handled by setting

$$\rho_{1*} - \frac{\rho_{2*}}{\cos^6 \frac{\vartheta'}{\sqrt{6}}} \cos \vartheta' - \frac{\rho_{1*}}{\cos^6 \frac{\vartheta'}{\sqrt{6}}} \cos (\vartheta' - 2\nu') +$$

$$\frac{\rho_{2*}}{\cos^6 \frac{\vartheta''}{\sqrt{6}}} \cos (\vartheta'' - 2\nu') + \frac{\rho_{1*}}{\cos^6 \frac{\vartheta''}{\sqrt{6}}} \cos (\vartheta'' - \nu_M) -$$

$$\frac{\rho_{1*}}{\cos^6 \frac{\vartheta_M}{\sqrt{6}}} \cos (\vartheta_M - \nu_M) = \frac{\sigma_M - \sigma_*}{2} \qquad (12)$$

provided it is assumed that

$$\left| DE \right| = \left| BC \right| = \rho_1' = \frac{\rho_{1*}}{\cos^6 \frac{\vartheta'}{\sqrt{6}}}$$

and

$$\left| GH \right| = \left| EF \right| = \rho_1'' = \frac{\rho_{1*}}{\cos^6 \frac{\vartheta''}{\sqrt{6}}}$$

In fact, one has in particular this time that

$$(BD)_y = - \frac{\rho_{2*}}{\cos^6 \frac{\vartheta'}{\sqrt{6}}} \cos \vartheta'$$

angle between $\overline{ED}$ and $y = (\overline{ED}, y) = \vartheta' - 2\nu'$

$$(EG)_y = \frac{\rho_{2*}}{\cos^6 \frac{\vartheta''}{\sqrt{6}}} \cos (\overline{EG}, y)$$

angle between $\overline{EG}$ and $y = (\overline{EG}, y) = \vartheta'' - 2\nu'$

angle between $\overline{GH}$ and $y = (\overline{GH}, y) = \vartheta'' - \nu_M$

and

$$(HL)_y = \frac{\rho_{1*}}{\cos^6 \frac{\vartheta_M}{\sqrt{6}}} \cos \psi_M$$

wherein the symbol ψ_M stands for $\vartheta_M - \nu_M$.

Numerical Applications

For illustrative purposes let us suppose that one wishes to design a tunnel which will reach a Mach number of

$$M = 2.5$$

by means of an effusor such as depicted in figure 6, or else with one with three kinks as in figure 8.

   Setting down the numerical values available to us, we get the following listing:

$$\psi_M = \text{arcos } \frac{1}{M} = 66^\circ \ 25.3'$$

$$\vartheta_M = \sqrt{6} \ \text{arctan} \ \frac{\tan \psi_M}{\sqrt{6}} = \sqrt{6} \ \text{arctan} \ \frac{\sqrt{M^2 - 1}}{\sqrt{6}} = 105^\circ \ 32.7'$$

$$\nu_M = 39^\circ \ 7.4'$$

$$\frac{\rho_M}{\rho_*} = \frac{1}{\cos^6 \dfrac{\vartheta_M}{\sqrt{6}}} = \left(\frac{5 + M^2}{6}\right)^3 = 6.5919$$

$$\frac{\sigma_M}{\sigma_*} = \frac{1}{M} \left(\frac{5 + M^2}{6}\right)^3 = 2.6368$$

   Let us compute the value of ν' which applies to the type of circular arc expansion incorporated into the figure 8 design. In this case if we let

$$\sigma_* = \rho_* = 1$$

$$\rho_1 = 0.5$$

$$\rho_2 = \rho_3 = 1$$

then, from equation (10), $\dfrac{\sigma_M - \sigma_*}{2} = 0.8184.$

Let the function $A(\vartheta')$ represent the left hand side of equation (10) (which is legitimate because v', v'', and ϑ'' are all functions of ϑ'), and we then propose to find the value of ϑ' which makes

$$A(\vartheta') = 0.8184 \tag{13}$$

In order to effect the solution of equation (13), the author made use of the method of approximation by secants (see fig. 10). Let us assume for example that ϑ_1' and ϑ_2' are two values of the independent variable which when substituted into the expression $A(\vartheta')$ renders a result which is too small in the first case and one which is too large in the second case in an attempt to find a value of ϑ' which makes equation (13) hold true. In addition, let ϑ_3' be a value of the independent variable which is much more accurate, and which can be obtained by linear interpolation. Then the two secants P_1 P_3 and P_2 P_3 will cut the horizontal line $A(\vartheta') = 0.8184$ in two points, which may be labelled S_1 and S_2. A better approximation to the exact solution of equation (13) is then obtained by selecting ϑ' as equal to a value ϑ_4 which falls within the interval defined by the end-points S_1 and S_2. After discarding one of the more distant points on the curve (in the case illustrated by fig. 10, the point ϑ_1' would be dropped) the whole process is repeated by working with the points P_2, P_3, and P_4 to start with again.

We shall try out this procedure by first selecting the value of ϑ' as = $60°$. Then one finds that:

$$\vartheta' = 60°$$

$$v' = 11.9°$$

$$v'' = 31.5°$$

$$\vartheta'' = 94.3°$$

$$A = 0.59 < 0.8184$$

The value of ϑ'' listed here is obtained by use of the relationship

$$v'' = \vartheta'' - \arctan\left(\sqrt{6}\,\tan\frac{\vartheta''}{\sqrt{6}}\right)$$

through use of the method of approximation based on interpolation along a tangent. According to this method, if a first approximate solution which is too large is determined and denoted by ϑ_1'' then a more accurate approximation to the exact value of ϑ'' is given by

$$\vartheta_2'' = \vartheta_1'' - \frac{v_1'' - v''}{\dfrac{dv''}{d\vartheta''}} = \vartheta_1'' - \frac{v_1'' - v''}{5}\left(6 + \cot^2\frac{\vartheta_1''}{\sqrt{6}}\right)$$

where the value of v_1'' is obtained by an analogous formula to the one given above for v''; i.e., here one uses the relation

$$v_1'' = \vartheta_1'' - \arctan\left(\sqrt{6}\,\tan\frac{\vartheta_1''}{\sqrt{6}}\right)$$

From the above derived numerical result it is seen that the guess $\vartheta' = 60°$ is a too small solution for equation (13). Consequently if the value $\vartheta' = 70°$ is now tried, it turns out that:

$$\vartheta' = 70°$$

$$v' = 16.9°$$

$$v'' = 36.5°$$

$$\vartheta'' = 101.7°$$

$$A = 1.47 > 0.8184$$

Thus the trial value $\vartheta' = 70°$ is a too large solution for equation (13). Linear interpolation then results in the value for ϑ' of 62.6°.

Consequently, using this value it results that:

$$\vartheta' = 62° 36'$$

$$\nu' = 13° 5'$$

$$\nu'' = 32° 39'$$

$$\vartheta'' = 96° 4'$$

$$A = 0.762 < 0.8184$$

Now continuing the computation to obtain a better approximation by means of the method outlined above (see fig. 10), one gets that

$$\vartheta' = 63° 20'$$

$$\nu' = 13° 26.7'$$

$$\nu'' = 33° 0.4'$$

$$\vartheta'' = 96° 36.9'$$

$$A = 0.8183$$

Consequently the solution of equation (13) is $\vartheta' = 63° 20'$ with an error which is less than 1 minute.

In carrying out the actual construction of the effusor contour it is necessary to point out that, if β is taken to denote the direction of the flow with respect to the x-axis, the following sign relationships hold:

$$d\beta = d\nu \text{ in the first (I) and last (III) expansion regions}$$
$$d\beta = -d\nu \text{ in the central (II) expansion region}$$

$$(14)$$

Now perform the integrations indicated by equations (14), substituting the proper limits, and one obtains

$$\left.\begin{array}{l} \beta = \nu \\[2mm] \beta = 2\nu' - \nu \\[2mm] \beta = \nu - \nu_M \end{array}\right\} \qquad (15)$$

in the regions I, II, and III, respectively.

If the coordinates of the points B, E, and H are assumed known, then the equations (15) afford the means of determining the coordinates of the point (x_1,y_1) which lies on the convex portion of the wall contour and which is related to an arbitrarily selected fixed value of the parameter ϑ. In addition, let the former equations (4) be modified to read

$$\left.\begin{array}{l} x_2 = x_1 + \rho \sin \alpha \\[2mm] y_2 = y_1 \mp \rho \cos \alpha \\[4mm] \rho = \rho_* \left(\cos \dfrac{\vartheta}{\sqrt{6}}\right)^{-6} \end{array}\right\} \qquad (16)$$

where the + sign in the second equation holds just for the central II region of expansion. These expressions, together with the equations (9), allow one to compute the coordinates (x_2,y_2) of the corresponding point lying on the concave portions of the wall.

Working with the illustrative case depicted in figure 9, let the starting data be selected, for example, as

$$\rho_* = 1 = \sigma_*$$

$$\rho_{1*} = 0.3$$

$$\rho_{2*} = \rho_{1*} + \rho_* = 1.3$$

Upon substitution of these values into equation (12), one will find that

$$B(\vartheta\,') = 0.8184 \tag{17}$$

Continuing the computation by an entirely analogous procedure as used previously, it is found that

$$\vartheta\,' = 63^{\circ}\ 5.7\,'$$

$$\nu\,' = 13^{\circ}\ 19.6\,'$$

$$\nu'' = 32^{\circ}\ 53.3\,'$$

$$\vartheta'' = 96^{\circ}\ 26.2\,'$$

In order to carry out the actual drawing of the effusor shape (see fig. 9) the relationships given as equations (9) are again employed and the results applying to the three convex portions of the wall will be given by, respectively:

$$x_1 = x_B + \rho_1 \sin \alpha$$

$$y_1 = y_B - \rho_1 \cos \alpha$$

$$x_1 = x_E + \rho_1 \sin \alpha$$

$$y_1 = y_E + \rho_1 \cos \alpha$$

$$x_1 = x_H + \rho_1 \sin \alpha$$

$$y_1 = y_H - \rho_1 \cos \alpha$$

where

$$\rho_1 = \frac{\rho_1{*}}{\cos^6 \dfrac{\vartheta}{\sqrt{6}}}$$

The determination of the concave portions of the wall is carried out in an analogous way, except for the mere replacement of the subscript 1 by the subscript 2.

CONCLUSIONS

The advantages accruing from the methods expounded here for design of the various kinds of effusor lie essentially in the great degree of precision with which it is possible to draw in the wall contour. A blemish of the method suggested for design of the effusors possessing three successive expansion regions (see figs. 8 and 9), which must be acknowledged, is that the length is longer than what would be found necessary if the effusor had been calculated according to the usual hodograph method, although the latter would be less exact (see fig. 11). The lengths of effusor, when non-dimensionalized by reference to the throat depth, have the following magnitudes in the cases exemplified by figures 8 and 9, respectively:

$$
\left.
\begin{array}{l}
\dfrac{l}{\rho_*} = 12.2 \\[3em]
\dfrac{l}{\rho_*} = 14.2
\end{array}
\right\}
\tag{18}
$$

The same ratio in the case of the effusor represented by figure 11 has the value 9.8, but it will be cut down to only 4.9 if the effusor shown in figure 11 is considered to be merely one half of a complete symmetric tunnel.

This defect in the effusors described here ceases to exist in the case of the skewed effusor designs first mentioned in this paper. These off-set designs can be fruitfully employed nevertheless where there is restricted room for the setup, because it should not entail a very great deal of trouble to incorporate a suitable compensating kink in the subsonic part of the tunnel.

A promising compromise design can be obtained by use of an effusor having two expansion regions (with equal and opposite amounts of turning). With this configuration it is clear that the working section will be lined up parallel with the axis of the throat section, except that it

will be offset laterally (see fig. 12). The length of the effusor and
its lateral displacement will have the following sizes, respectively

$$\left. \begin{array}{c} \dfrac{l}{\rho_*} = 9.7 \\[2em] \dfrac{s}{\rho_*} = 1.4 \end{array} \right\} \tag{19}$$

As is evident, this displacement s/ρ_* is not of formidable size,
while on the other hand the length of the effusor has been somewhat
reduced, in comparison with the cases illustrated in figures 8 and 9.

Despite all that has been said, it is still worthy of note that in
the case of effusors designed for Mach numbers which are only slightly
greater than unity; that is, for effusors whose lengths do not exceed
that of the working section, the effusor designed with three expansion
regions can still be employed to good purpose. Such an effusor designed
to produce a Mach number of $M = 1.2$ is illustrated in figure 13.
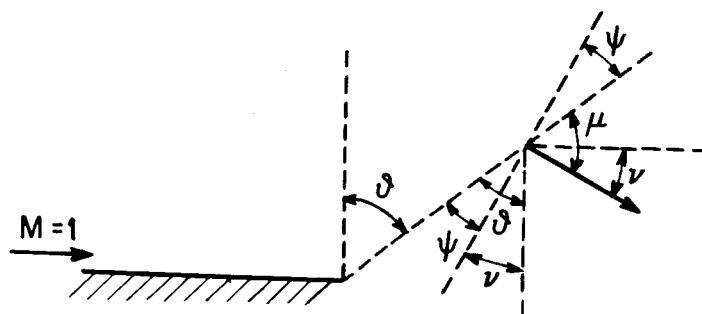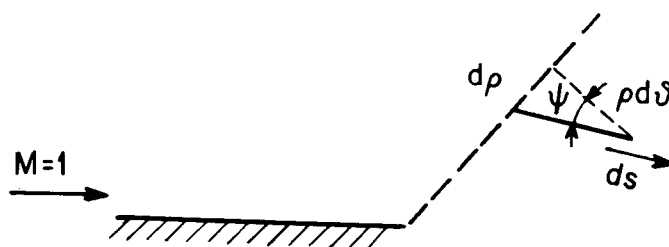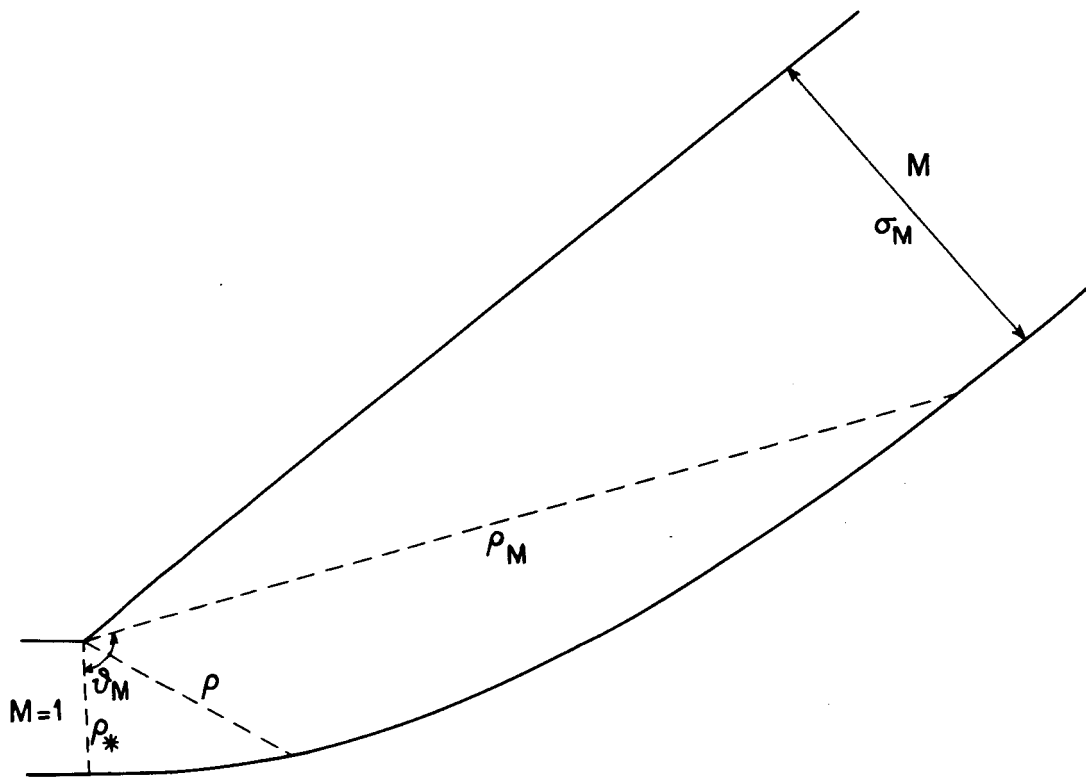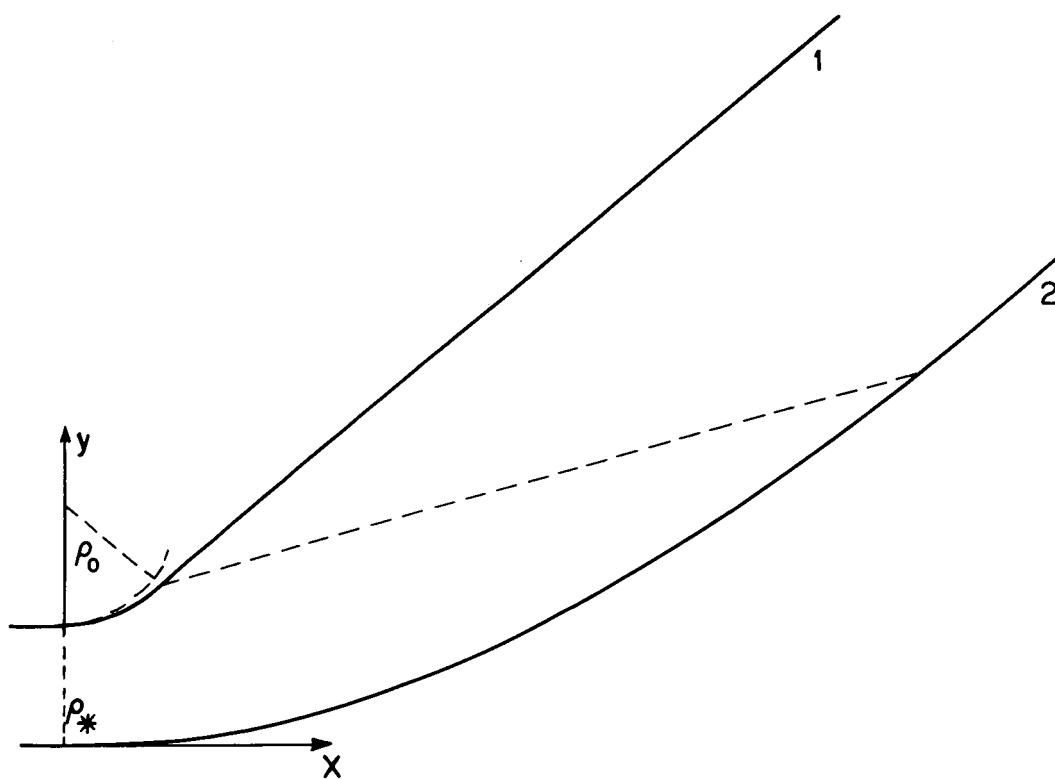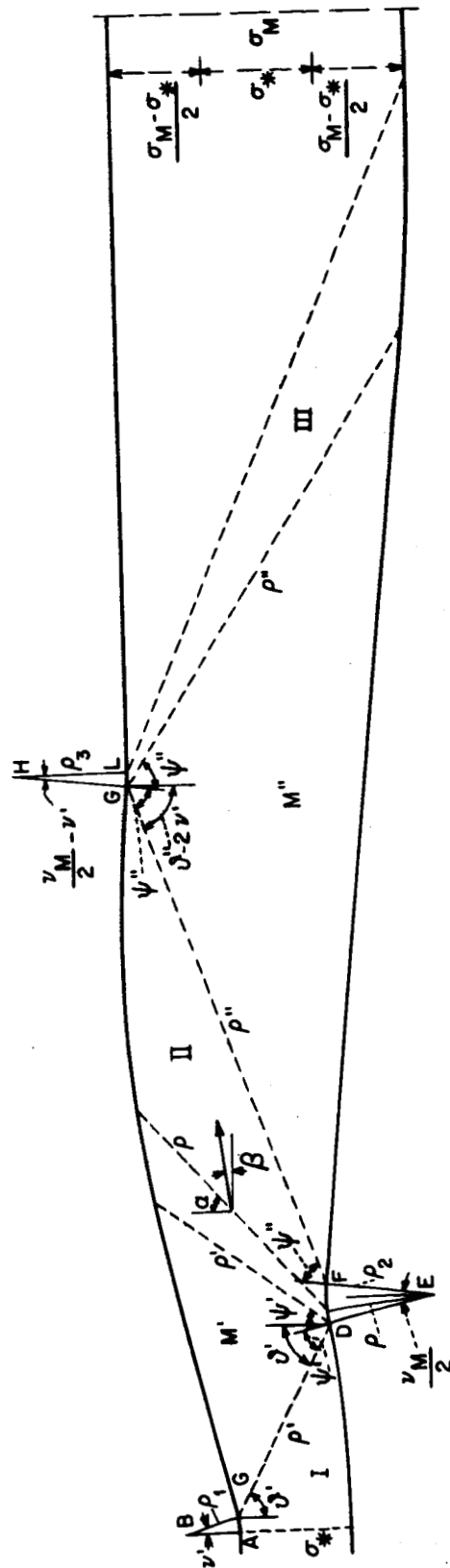
Figure 1
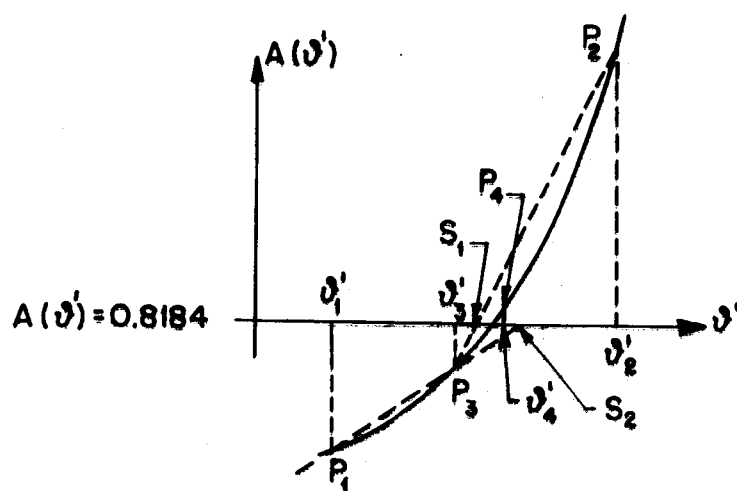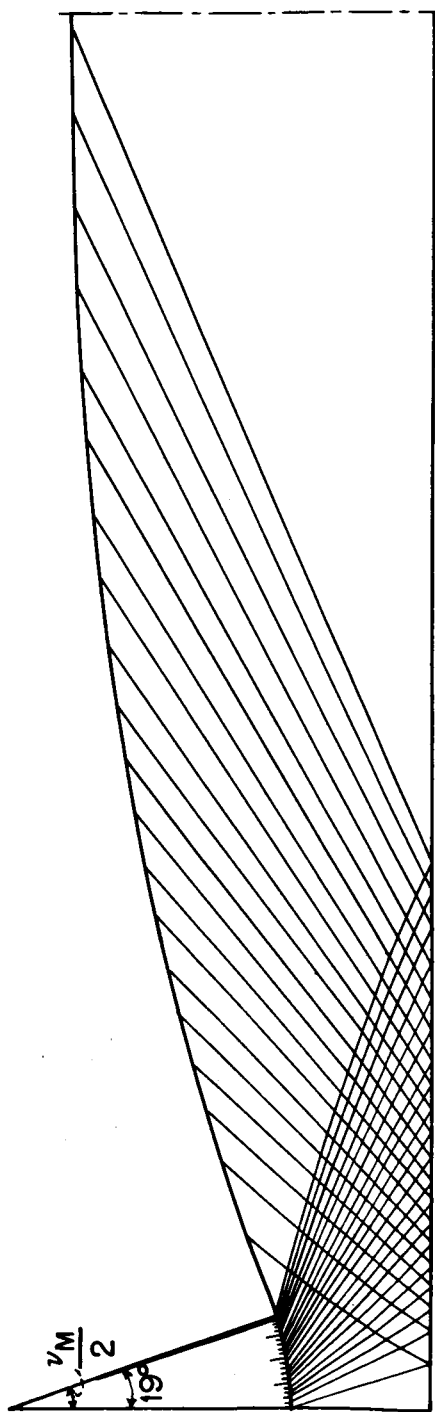

Figure 2

Figure 3
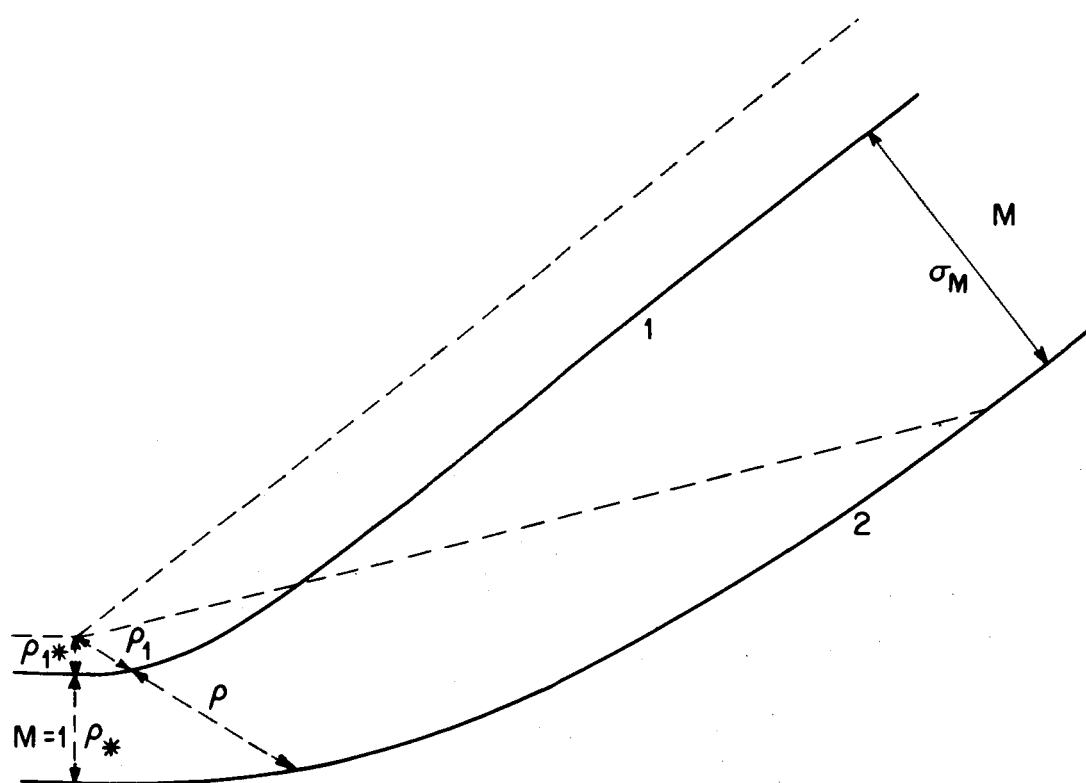
Figure 4
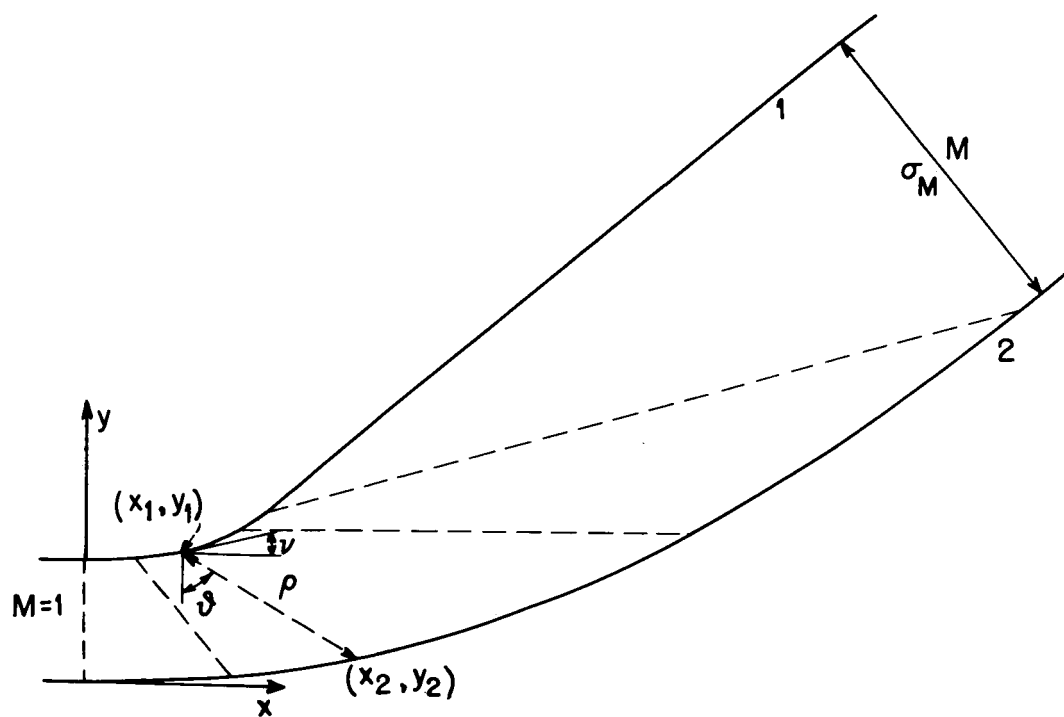
Figure 5

Figure 6

Figure 7

Figure 8

Figure 9

Figure 10

Figure 11

Figure 12

Figure 13